


Open Access

<https://doi.org/10.48130/fia-0025-0002>

Food Innovation and Advances 2025, 4(1): 31–42

miR395-APS1 modulates grape resistance to *Botrytis cinerea* through the sulfur metabolism pathway

Yizhou Xiang^{1#}, Hemaoyuan^{1#}, Chao Ma², Dong Li¹, Qiannan Hu¹, Yingying Dong¹, Miroslava Kačániová³,
Zhaojun Ban⁴, Bin Wu^{5*} and Li Li^{1,6*} ¹ College of Biosystems Engineering and Food Science, Fuli Institute of Food Science, Key Laboratory of Agro-Products Postharvest Handling, Ministry of Agriculture and Rural Affairs, Zhejiang University, Hangzhou 310058, China² Department of Plant Science, School of Agriculture and Biology, Shanghai Jiao Tong University, Shanghai 200240, China³ Institute of Horticulture, Faculty of Horticulture and Landscape Engineering, Slovak University of Agriculture, Nitra 949 76, Slovakia⁴ School of Biological and Chemical Engineering, Zhejiang University of Science and Technology, Hangzhou 310023, China⁵ Institute of Agro-products Storage and Processing & Xinjiang Key Laboratory of Processing and Preservation of Agricultural Products, Xinjiang Academy of Agricultural Science, Urumqi 830091, China⁶ National-Local Joint Engineering Laboratory of Intelligent Food Technology and Equipment, Zhejiang Key Laboratory for Agro-Food Processing, Zhejiang Engineering Laboratory of Food Technology and Equipment, Zhejiang University, Hangzhou 310058, China

Authors contributed equally: Yizhou Xiang, Hemaoyuan

* Corresponding authors, E-mail: 42042615@qq.com; lili1984@zju.edu.cn

Abstract

MicroRNAs (miRNAs) play important roles in various physiological activities in plants. However, their role in protecting grapes against gray mold (*Botrytis cinerea*) invasion remains largely unexplored. This study focuses on the phenotypic and physiological responses of 'Shine Muscat' (*Vitis vinifera* × *V. labrusca*) to gray mold infestation. High-throughput sequencing implicates several miRNAs, including miR398 and miR319, involved in the plant's defense mechanisms. Notably, miR395 emerges as a key player, positively influencing grape disease resistance. Specifically, miR395 downregulated the expression of its target gene *APS1*, which encodes ATP sulfurylase, a crucial enzyme in the plant's sulfur metabolic pathway. Concurrently, ATP sulfurylase downregulation increased the content of sulfate ions and glutathione (GSH). These findings were corroborated by our study of *APS1*. Collectively, these results suggest that miR395-*APS1* modulates sulfur metabolism in grapes, thereby enhancing resistance to *B. cinerea*. The observed miRNA-mediated interactions between grapes and *B. cinerea* elucidate the role of miR395 in grape resistance to gray mold and offer new insights into the molecular mechanisms of grape disease resistance.

Citation: Xiang Y, Yuan H, Ma C, Li D, , et al. 2025. miR395-*APS1* modulates grape resistance to *Botrytis cinerea* through the sulfur metabolism pathway. *Food Innovation and Advances* 4(1): 31–42 <https://doi.org/10.48130/fia-0025-0002>

Introduction

Grape (*Vitis vinifera*) is a globally cultivated and highly profitable crop valued for its rich nutritional content^[1]. Among the many grape varieties, 'Shine Muscat' (*Vitis vinifera* × *V. labrusca*) has gained immense popularity among consumers due to its exquisite taste and distinctive rose aroma^[2]. Despite its widespread cultivation, covering more than 800,000 hectares globally^[3], 'Shine Muscat' is particularly vulnerable to pathogen attacks, primarily attributed to its high moisture content. This susceptibility highlights the critical need to explore the fruit's intrinsic defense mechanisms and phenotypic traits to devise more effective strategies for disease management^[4,5].

Botrytis cinerea is a necrotrophic plant pathogen responsible for gray mold, one of the most devastating diseases affecting grape production worldwide^[6,7]. This pathogen inflicts severe damage across all stages of the grape industry, including cultivation, production, logistics, and marketing^[8]. As a result, there has been growing research interest in recent years aimed at preventing gray mold in grapes. For instance, Zhang et al. demonstrated that chitosan treatment reduced gray mold damage by upregulating genes related to the jasmonic acid (JA) pathway, thereby enhancing disease^[9]. Similarly, exogenous N₂O treatment was found to promote the expression of key genes in the phenylpropanoid metabolic pathway and

increase the accumulation of total phenolics and flavonoids, bolstering resistance to gray mold^[10]. Transcriptomic and metabolomic analyses by Song et al. revealed that sodium nitroprusside treatment elevated the levels of resveratrol and other antioxidant-associated compounds through the stilbene synthesis pathway, protection against oxidative damage^[11]. Moreover, exogenous phenolic treatments have also been shown to improve grape resistance to *B. cinerea*^[12]. Notably, gray mold infection induces significant changes in grape phenotypic characteristics, which can serve as indicators for evaluating plant resistance to the disease^[13]. However, despite these advancements, most studies on gray mold management focus on exogenous treatments, leaving a critical gap in understanding the intrinsic resistance mechanisms of grapes against this pathogen.

MicroRNAs (miRNAs) are small endogenous RNA molecules, typically 21–24 nucleotides in length, that play crucial regulatory roles in plants. Extensive research has revealed their involvement in responses to both biotic and abiotic stresses^[14,15]. With growing interest in miRNAs, mounting evidence underscores their key role in modulating plant-pathogen interactions^[16]. For instance, Yang et al. demonstrated that in rice, miR395 negatively regulates *OsAPS1* and two sulfate transporter genes, leading to sulfate accumulation. This subsequently reduces extracellular polysaccharide production and biofilm formation in pathogens, thereby enhancing rice resistance to bacterial infections^[17]. Similarly, overexpression of miR394 in

Arabidopsis was found to downregulate the *LCR* gene, resulting in decreased resistance of *B. cinerea*^[18]. Through validation in *Arabidopsis*, miR319c was shown to target the *TCP29* gene, acting as a positive regulator of tomato resistance to *B. cinerea*^[19]. Furthermore, overexpression of *Arabidopsis* miR399f increased resistance of necrotrophic (*Plectosphaerella cucumerina*) and hemibiotrophic (*Colletotrichum higginsianum*) fungal pathogens by downregulating the *PHO2* gene^[20]. However, there are relatively few studies concerning the role miRNA plays in the resistance mechanisms of grape to gray mold.

To clarify the phenotypic and metabolic changes of *Vitis vinifera* × *V. labrusca* grapes upon infection by *B. cinerea*, and to understand the miRNAs involved in this host-pathogen interaction, we detected the expression changes of redox, metabolic, and disease-resistance related genes of 'Shine Muscat' after *B. cinerea* inoculation. Through miRNA sequencing, we identified both the miRNAs involved in this interaction, as well as the gene expression targets of the miRNAs used in the grape-*B. cinerea* interaction, and the targets of miRNAs degradation group sequencing. The function of miRNA was verified using molecular biology techniques. This study provides a comprehensive perspective on the role of miRNAs in grape resistance to *B. cinerea* by analyzing the phenotypic and molecular changes in grapes infected with gray mold, offering new insights into the mechanisms of disease resistance and strategies to reduce the occurrence of gray mold.

Results

Physiological responses, production, and scavenging of ROS of grapes inoculated with *B. cinerea*

As shown in Fig. 1a, at 72 h after *B. cinerea* inoculation, all grapes began to exhibit distinct brown lesions around the inoculation site, a typical necrotrophic phenotype. From 72 h onwards, these brown lesions expanded rapidly, signaling the progression of the disease. At 120 h, obvious aerial hyphae emerged at the necrotic sites of some grapes, and all necrotic sites had developed an unconsolidated, soft texture, with conspicuous gray mold mycelium visible (Fig. 1a), indicating that the gray mold had nearly completed the colonization of the grapes.

To quantify the extent of necrosis, we measured the diameter of the lesions at the necrotic sites. The results demonstrated that from 72 h onward, the lesion diameter began to increase, showing an extremely significant difference relative to the control starting from 72 h (Fig. 1b). This suggests a rapid spread of the gray mold condition during this stage. At 120 h, the lesion diameter reached its maximum size during the observed period. Correspondingly, at this stage, the necrotic site exhibited new phenotypes such as tissue softening collapse, exudation of tissue fluid, deepening of

color, and increased number of hyphae (Fig. 1a). These observations indicate that the colonization of *B. cinerea* was essentially completed by this time.

The antioxidant responses to *B. cinerea* inoculation are summarized in Fig. 2. The H₂O₂ content in both the *B. cinerea* treated and control groups showed an increasing trend, but from 24 h onwards, the H₂O₂ content of the treated group increased sharply and reached a maximum at 120 h, showing a high significant difference relative to the control group during this period ($p < 0.005$). Additionally, the superoxide anion concentration in the treated group showed a significant increase from 24 h onwards, reaching a maximum at 120 h. These levels were significantly higher than the control group at this stage ($p < 0.05$). The changes in MDA were investigated. After inoculation, starting from 12 h, the MDA levels in the treated group gradually increased, reaching a peak at 72 h. These levels were significantly higher relative to the levels in the control group at 120 h ($p < 0.005$). Besides, the contents of GSH and GSSG were also measured. After inoculation, the GSH content increased in both the treated and control groups. Although the differences were not statistically significant, the content in the treated group was higher than that of the control group in each period. As for GSSG, at 120 h, the content in the treated group was significantly higher compared to the control group ($p < 0.05$). Notably, there was no consistent trend differentiating the GSH and GSSG contents between the treated and control groups throughout the observation window.

To investigate the changes in antioxidant-related enzyme activities after inoculation, we examined the enzyme activities of CAT, APX, and SOD, as well as the expression of their corresponding genes. After inoculation, no significant difference was shown in CAT activity between the treated and control groups. Despite the minimal difference in CAT activity, compared to the control group, the expression level of the gene *CAT* was higher in the treated group at 12 and 24 h (Fig. 3), but significantly lower than in the control group at the rest of the period ($p < 0.05$). The APX enzyme activity of grapes inoculated with *B. cinerea* showed an overall trend of first increasing to a peak at 6 h, and then decreasing. Compared to the control group, the APX activity of the treated group was higher up to 6 h and then lower than the control afterward, with significant differences from the control group at 3 and 24 h ($p < 0.05$). The expression levels of the *APX* gene in the treated group similarly showed no clear trend over time vs the control group (Fig. 3), with significant differences from the control at 6–72 h ($p < 0.005$). As for SOD, the trends of SOD activity changes were similar in the treated and control groups, with the levels in the treated group gradually increasing in the early stages and followed by a decrease. Its related gene, *CSD6*, coding Cu/Zn superoxide dismutase, and *MSD2*, coding Mn superoxide dismutase, were both significantly higher in the treatment group at 12 h ($p < 0.01$), and significantly lower at 72 h (Fig. 3, $p < 0.005$).

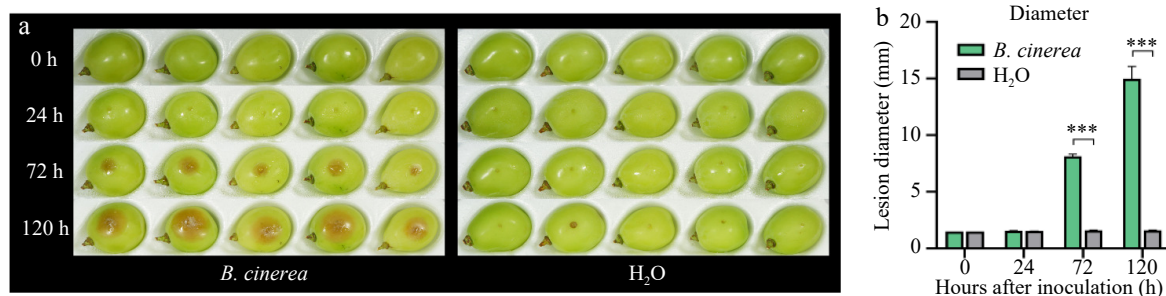


Fig. 1 (a) Necrotrophic phenotype, and (b) lesion diameter of grapes after *B. cinerea* inoculation. Three biological replicates were performed for each group of five grapes.

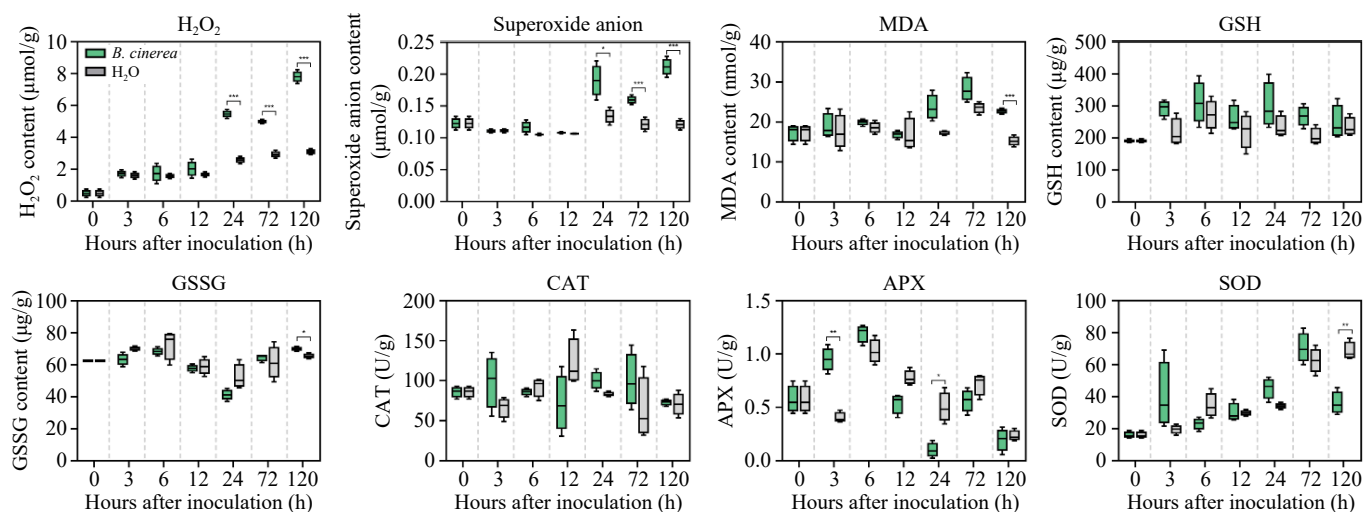


Fig. 2 Contents of H₂O₂, superoxide anion, MDA, GSH, GSSG, and the antioxidant related enzymes activity of CAT, APX, and SOD.

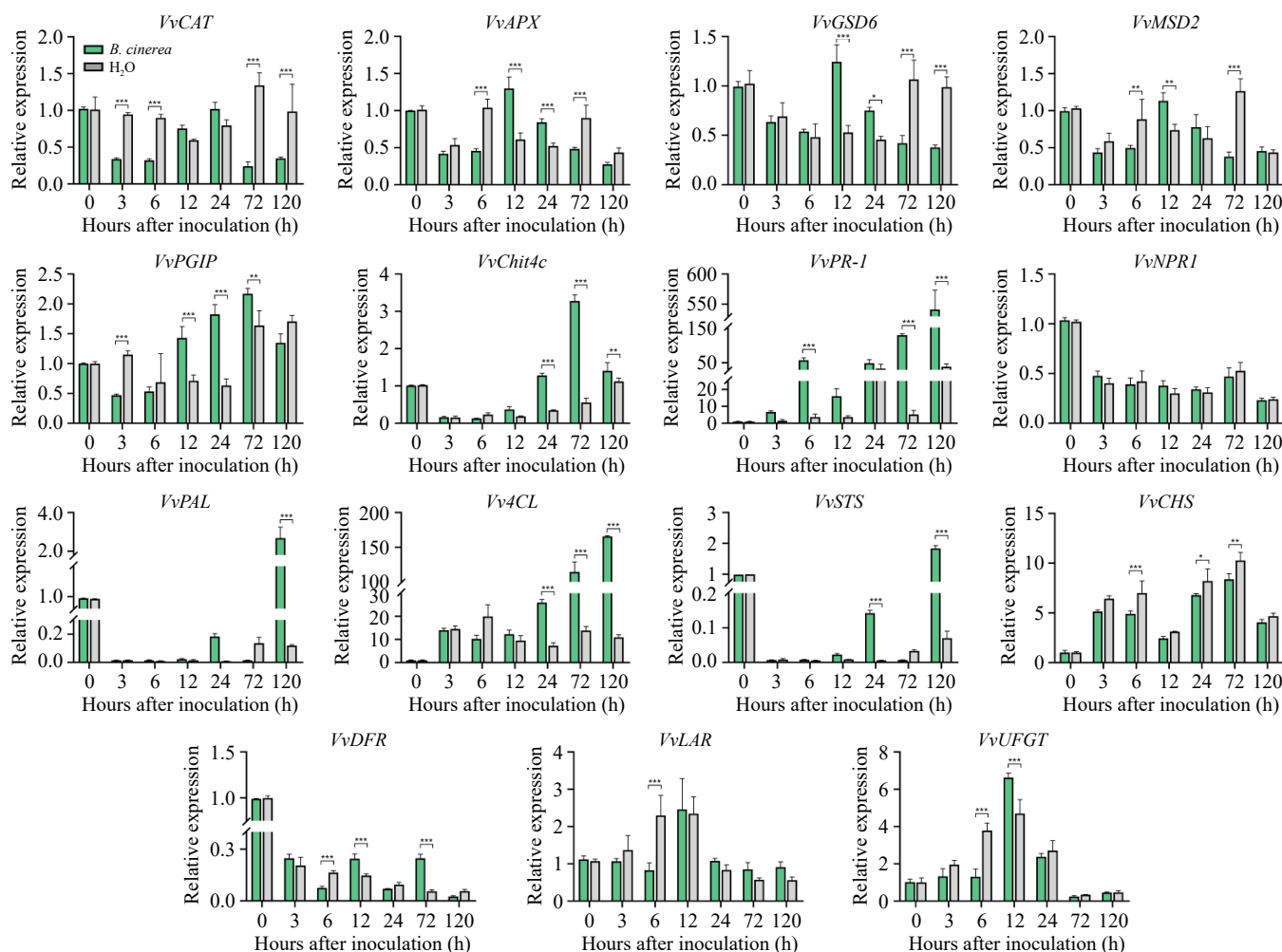


Fig. 3 Expression of genes coding for key antioxidant enzymes, and genes involved in pathogen response, and phenylpropane metabolism genes in grapes.

Changes of gene expression related to pathogen response and phenylpropane metabolism pathway after inoculation

Pathogenic response genes participate in the resistance process (Fig. 3). *PGIP*, encoding fungal polygalacturonase-inhibiting protein, showed an increasing trend in the treatment group and was

significantly higher compared to the control group at 12, 24, and 72 h ($p < 0.01$). Similarly, *CHIT4c*, the gene encoding an acidic class IV chitinase, was significantly higher in the treated group relative to the control at 24, 72, and 120 h, peaking at 72 h ($p < 0.01$). The *PR-1* gene plays a vital role in plant-pathogen interactions. In the treated group, its expression level showed an increasing trend and was

significantly higher compared to the control at 6, 72, and 120 h ($p < 0.005$). However, there was no significant difference in the expression of the *NPR1* gene between the treated and control groups.

Phenylpropane metabolic pathway genes are upregulated during the resistance process. Compared to the control group, the expression level of *PAL* in the treated group was significantly higher at 120 h ($p < 0.005$). Similarly, the expression level of 4-coumaroyl-coA synthase (*4CL*) was significantly higher relative to the control starting from 24 h ($p < 0.005$), and the expression level of the stilbene synthase (*STS*) gene was also significantly higher relative to the control at 24 and 120 h ($p < 0.005$). In the flavonoid pathway, in the treated group, the expression level of chalcone synthase (*CHS*) was lower relative to the control group at each stage, with significant differences at 6, 24, and 72 h ($p < 0.05$), dihydroflavonol reductase (*DFR*) showed a decreasing trend in both the treated and control groups. Both *LAR* and *UFGT* showed an increasing trend followed by a decreasing trend, with both having maximum expression levels at 12 h.

In addition, the expression of two key genes of the JA pathway, COR-insensitive 1 (*COI1*) and lipoxygenase (*LOX*), were also measured (Supplementary Fig. S1a & b). In the treated group, the expression level of *COI1* was significantly higher relative to the control at 12 and 24 h ($p < 0.005$). Additionally, the expression levels of genes related to cell wall degradation were also measured, as shown in Supplementary Fig. S1c–e. Compared to the control group, polygalacturonase 1 (*PG1*) and pectin methylesterase 1 (*PME1*) expression levels in the treated group were significantly higher at 120 h ($p < 0.005$) and 3, 6, and 24 h ($p < 0.05$), respectively. Expression levels of the pectin methylesterase 2 (*PME2*) gene did not show significant differences relative to control over the observation period.

Analysis of miRNA sequencing of grapes inoculated with *B. cinerea*

To study the miRNAs involved in the interaction between 'Shine Muscat' and *B. cinerea*, grapes from day 3 of the treated and control groups were selected for miRNA analysis, consisting of six miRNA libraries (two different treatments \times three replicates). A total of 15,331,902 (TR) and 12,271,339 (CT) clean reads were obtained, respectively (Supplementary Table S2). The most common fragments had a length of 21 nt, which accounted for about 26.84% and 28.19% of the treated and control libraries, respectively (Fig. 4a). A total of 96 known mature miRNAs in this species from 42 families were identified based on sequence similarity using the miRBase database (Supplementary Table S3). After analyzing the homology of known sequences across other species, a total of 129 conserved miRNAs were conserved across 25 different species, of which the most significant proportion was *Glycine max*, which contained 30.23% of the conserved miRNAs screened in this analysis (Supplementary Table S4). In addition, a total of 146 putative novel miRNAs were identified using ACGT101-miR (Supplementary Table S5). The differentially expressed miRNAs are shown in Fig. 4b. The GO enrichment results are shown in Fig. 4c. The dominant biological processes identified were those involved with the regulation of transcription, oxidation-reduction process, and protein phosphorylation. In terms of cellular components, the dominant categories were membrane, integral components of the membrane, and nucleus. The primary molecular function categories were protein binding, ATP binding, and DNA binding. Furthermore, the KEGG enrichment results are shown in Fig. 4d, the significantly enriched KEGG pathways mainly include riboflavin metabolism, sulfur relay system, and peroxisome pathways. Notably, riboflavin metabolism is closely related to energy metabolism and redox homeostasis in plants, whereas the sulfur relay system is related to the transfer of sulfur-containing material production.

Target gene identification for miRNAs by degradome sequencing

To better clarify the function of miRNAs in grape-*B. cinerea* interaction, we analyzed the targets of miRNAs in grapes by constructing two degradome libraries for the treated and control groups, as shown in Supplementary Table S6 and S7. A total of 302 potential targets were identified.

The KEGG enrichment results previously identified upregulation of the sulfur relay system, which led us to focus on miRNAs related to sulfur metabolism. The high-throughput sequencing results showed that miR395 participates in grape-*B. cinerea* interactions, which has been shown in many studies to be closely related to sulfur metabolism. This result prompted us to focus on the biological function of miR395. Because the mode of action of miRNAs on their target genes is mainly cleavage, we identified the candidate target gene *APS1* of miR395 by degradome sequencing (Fig. 4f) and further investigated their trends after gray mold inoculation by qRT-PCR experiments and identified the cleavage sites through 5' RACE experiments, shown in Fig. 4e & g, respectively. Sequencing verification of *APS1* mRNA cleavage by 5' RACE experiment revealed that the cleavage site coincided with the miR395 target (Fig. 4g). Meanwhile, qPCR experiments showed that after inoculation, miR395 steadily increased to its highest value at 12 h. The expression of miR395 gradually began to decline to a minimum at 72 h and then slightly increased at 120 h (Fig. 4e). Expression levels of *APS1* did not change significantly from 0–24 h after inoculation and showed a significant increase in relative expression at 72 and 120 h, negatively corresponding to the decreasing trend over the same period (Fig. 4e). From these results, we concluded that *APS1* is the target gene of miR395.

Verification of the function of vvi-miR395I in the resistance against *B. cinerea* in grapes and *Nicotiana benthamiana*

To initially validate the biological function of vvi-miR395 under gray mold stress, we constructed miR395-OE and STTM395 vectors by Nimble Cloning, they were transiently expressed in *N. benthamiana* leaves respectively. miR395-OE as the overexpression group, STTM as the silencing group, and empty vector (EV) as the control. In the overexpression group, the expression of miR395 was about 160-fold higher compared to the control. In contrast, compared to the control, the expression of miR395 was 0.5-fold lower in the silencing group, as expected. Besides, the expression levels of pathogen response-related genes were also examined (Supplementary Fig. S2a). Compared to the control group, the expression of disease process-related proteins *PR1*, *PR2*, *PR4*, and *PR5* all showed significantly higher expression: 4.8, 1.5, 1.8, and 1.2 times higher in the overexpression group, respectively. Likewise, the expression levels in the silencing group were reduced by 45%, 70%, 55%, and 75%, respectively, compared to the control. Based on these results, we hypothesized that miR395 could induce the expression of *PRs* to regulate tobacco disease resistance. Furthermore, we examined the phenotypic disease resistance of transiently transformed leaves of *N. benthamiana* by observing the leaves 5 d after inoculation with gray mold spores, as shown in Supplementary Fig. S2b. Compared to the control, the size of leaf spots was significantly smaller in the overexpression group. The results of Trypan Blue staining also showed a lower number of dead cells (Supplementary Fig. S2b). In contrast, the silencing group was more severely infected (as observed by larger lesions) than the control group and presented a higher number of dead cells. These results suggest that transient overexpression of vvi-miR395 in *N. benthamiana* increased the resistance of tobacco to gray mold while silencing increased the susceptibility of tobacco to infection.

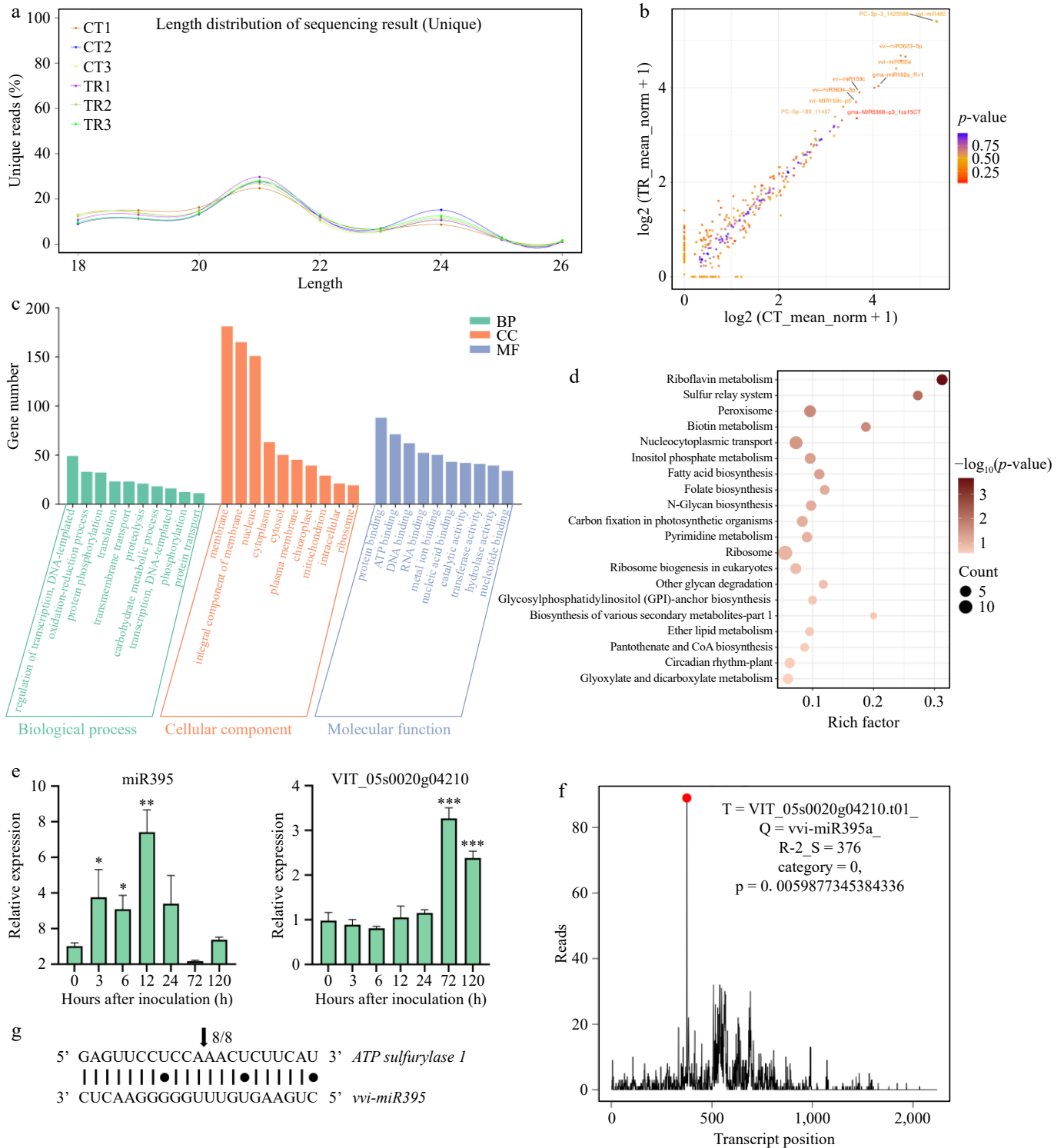


Fig. 4 MiRNA omics analysis of grape response to *B. cinerea*. (a) Length and size distribution of unique sequences in sRNA libraries in grape. (b) Scatter map of miRNA differentially expressed between samples. (c) GO enrichment analysis of DE miRNA target genes. (d) KEGG enrichment analysis of DE miRNA target genes. (e) Relative expression level of miR395 and their target genes of grape inoculated with *B. cinerea* by qRT-PCR, compared to 0 h. (f) Target plot of the target cleaved by the miR395. Cleavage features in *VvAPS1* mRNA by miR395 from the degradome library. (g) Sequence alignment of miR395 sequence with the complementary sequence of its target transcript.

In the transiently transformed grapes, a gray mold inoculation experiment was conducted, and after 5 d post-inoculation, we observed the physical characteristics of the grapes. Compared to the control, the phenotypic results showed significantly smaller lesion diameters in the overexpression group ($p < 0.005$) and significantly larger lesions in the silencing group ($p < 0.01$) (Fig. 5a). Besides, we

examined the content of some sulfur-containing metabolites in grapes after transient transformation (Fig. 5b). Among them, compared to the control group, SO_4^{2-} content was significantly higher in the overexpression group ($p < 0.01$), and significantly lower in the silencing group ($p < 0.005$). GSH content was significantly higher in the overexpression group ($p < 0.05$), though no

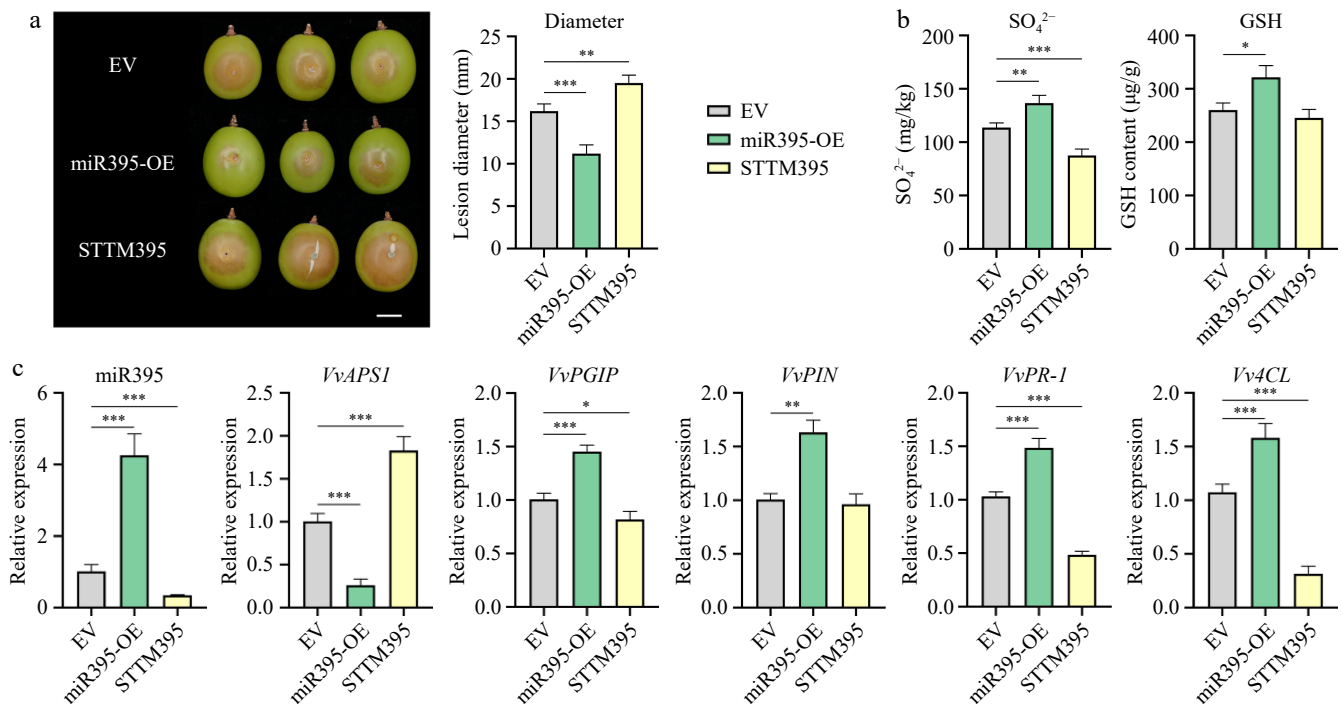


Fig. 5 Verification of the function of vvi-miR395 in 'Shine Muscat' grape. (a) Necrotrophic phenotype and lesion diameter of grapes caused by *B. cinerea* after transient transformation with miR395. Three biological replicates were performed for each group of five grapes. Scale bars correspond to 10 mm. (b) Content of SO_4^{2-} and GSH in grapes after transient transformation with miR395. (c) Relative expression level of miR395 and its target gene and pathogen response-related genes in grapes after transient transformation with miR395.

significant difference was observed in the silencing group, the mean value was smaller compared to the control (Fig. 5b). Notably, there were no significant differences in the contents of SO_3^{2-} and Cys in the overexpression group, silencing group, and control (Supplementary Fig. S3a). Besides, compared to the control, the expression of miR395 was higher in the overexpression group ($p < 0.005$) and lower in the silencing group ($p < 0.005$); the opposite was true for the expression of the target gene *APS1*, which was lower in the overexpression group ($p < 0.005$) and higher in the group ($p < 0.005$) (Fig. 5c). Again, this relationship emphasizes that miR395 acts as a repressor towards *APS1* expression. In the expression level of pathogen response-related genes, the expression levels of *PR-1*, *PGIP*, and *4CL* were all higher in the overexpression group ($p < 0.005$) and lower in the silencing group ($p < 0.05$) (Fig. 5c). However, no expected difference was shown in the expression levels of *PR2* and *PAL* (Supplementary Fig. S3b).

In summary, we demonstrate that miR395 can participate in the expression of genes related to pathogen response and in sulfur metabolism-related pathways, thus positively regulating grapevine disease resistance. This led us to focus on the physiological function of its target gene, *VvAPS1*, in grapevine resistance to gray mold invasion.

VvAPS1 functions in sulfate metabolism to modulate grape resistance against *B. cinerea*

The amino acid sequence of the *VvAPS1* protein was predicted to be localized in chloroplasts. To verify this hypothesis, we observed the transient transformation of a construct encoding the *VvAPS1*-GFP fusion protein into tobacco leaves. *VvAPS1*-GFP was found to co-localize within the chloroplast's fluorescence (Fig. 6a). After the transient transformation of *VvAPS1*, we also measured the lesion diameter of grapes, as shown in Fig. 6b. Compared to the control, the lesion diameters of grapes were significantly larger in the

overexpression group ($p < 0.01$), and significantly smaller in the silencing group ($p < 0.005$).

To clarify the impact of *VvAPS1* on grape sulfur metabolism, we measured the content of sulfur-containing metabolites in grapes after the transient transformation of *VvAPS1* (Fig. 6c). Compared to the control, both the SO_4^{2-} and GSH content were significantly higher in the silencing group ($p < 0.05$), while in the overexpression group, only SO_4^{2-} was significantly lower ($p < 0.005$) (Fig. 6c). Though there was no significant difference in the overexpression group, GSH content was slightly lower than the control (Fig. 6c). Despite the changes in SO_4^{2-} and GSH levels from differential expression of *VvAPS1*, the SO_3^{2-} and Cys contents in the overexpression and silencing groups showed no significant difference compared to the control (Supplementary Fig. S4a). The expression level of the sulfur metabolism-related genes was measured in response to overexpression or silencing of *VvAPS1* (Fig. 6d & Supplementary Fig. S4b). In particular, the *GS* gene is a key component in the production of GSH. Compared to the control, *GS* expression was significantly lower in the overexpression group (Fig. 6d), while in the silencing group, the expression level was significantly higher (Fig. 6d). These observations are consistent with the measured GSH content under similar conditions. Additionally, we also detected the expression level of pathogenic response-related genes (Fig. 6d & Supplementary Fig. S4b). Compared to the control, the *PGIP*, *PIN*, *PR-1*, and *4CL* genes were significantly lower in the overexpression group, while in the silencing group, they were significantly higher relative to the control. These results suggest that *VvAPS1* negatively regulated the resistance of grapes to gray mold via the regulation of these pathogenic response genes.

These results suggest that the target gene of miR395, *VvAPS1*, is involved in the sulfur metabolism pathway, which can negatively regulate the content of SO_4^{2-} in grapes and, to a lesser extent, negatively regulate the content of GSH. *VvAPS1* also appears to be

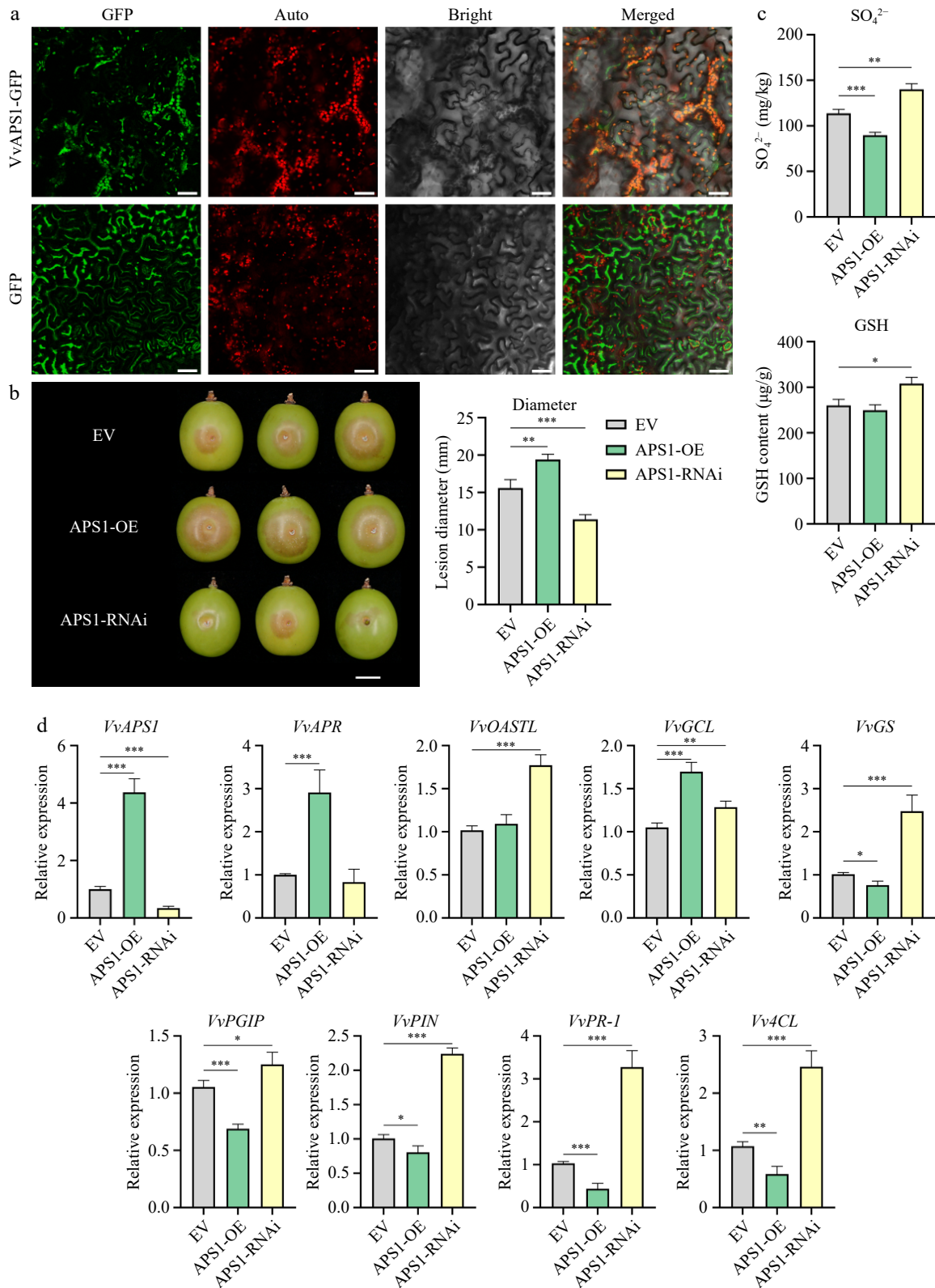


Fig. 6 Verification of the function of *VvAPS1* in 'Shine Muscat' grape. (a) Analysis of *VvAPS1* subcellular localization in tobacco leaf. Scale bars correspond to 50 μm. (b) Necrotrophic phenotype and lesion diameter of grapes caused by *B. cinerea* after transient transformation with *VvAPS1*. Three biological replicates were performed for each group of five grapes. Scale bars correspond to 10 mm. (c) Content of SO₄²⁻, and GSH in grapes after transient transformation with *VvAPS1*. (d) Relative expression level of *VvAPS1*, sulfur metabolism-related genes, and pathogen response-related genes in grapes after transient transformation with *VvAPS1*.

involved in the regulation of pathogen-responsive gene expression, which negatively affects the resistance of grapes to *B. cinerea*.

Discussion

'Shine Muscat' phenotypic change and loss of redox homeostasis upon *B. cinerea* infection

Upon stimulation by microorganisms (pathogens), plants modulate the immune system for plant immunity through multiple pathways, most commonly using an oxidative burst of increased ROS levels. In the present study, we observed phenotypic changes in grapes after inoculation with *B. cinerea*, as well as redox-related metabolic changes in tissues. Physiologically, we found that lesions appeared at 72 h after inoculation and expanded rapidly from then on (Fig. 1a), indicating the massive death of grape cells from now on as a manifestation of immune regulation. Supporting the involvement of immune regulation, the ROS-related molecules H_2O_2 and $O_2^{\cdot -}$ began to significantly increase 24 h after inoculation, signifying a ROS burst. The accumulation of GSH protects the membrane. Meanwhile, the content of GSH decreased, the content of GSSG relatively increased, and the content of MDA significantly increased at the late stage of inoculation, indicating that the cell membrane was severely damaged. While in the assay of antioxidant enzymes, the activities of CAT and APX were relatively high in the early stage (0–24 h), with a significant difference in SOD active matter, and after that, the activity of SOD dominated, which may have caused the accumulation of H_2O_2 in the late stage. It is suggested that the accumulation of ROS caused by pathogenic bacterial attack has an important role for plants^[21,22]. We speculate that H_2O_2 may be involved in the immune regulation of grapes as a signaling molecule at this stage. Furthermore, we observed a negative correlation between APX enzyme activity and gene expression at 3, 12, and 24 h post-treatment. This could result from post-transcriptional regulation, where mRNA levels do not directly translate into enzyme activity due to factors like enzyme stability, availability of cofactors, and temporal delays between transcription and enzyme activation. These findings suggest that enzyme activity in response to *B. cinerea* infection is modulated by complex, multi-level regulatory mechanisms.

Phenylpropane metabolic pathway and pathogen response-related genes involved in *B. cinerea* interactions

The main modes of plant immune response are pattern-triggered immunity (PTI) and effector-triggered immunity (ETI), in which PTI is mainly a non-specific basal defense response, while ETI is mainly a specific defense response through the recognition of pathogen effector proteins by *R* genes^[23]. It has been shown that the joint regulation of PTI and ETI regulates the immune response of plants under pathogenic invasion. We investigated the expression of several pathogen response-related genes, *PGIP*, *NPR1*, *PR-1*, and *PR2*, after inoculation. We found that *PGIP*, encoding a polygalacturonase-inhibiting protein, had significantly higher expression starting at 12 h in response to the infiltration of *B. cinerea*. It was shown that *NPR1*, a key regulator of SAR, promotes the expression of downstream *PR* genes^[24], though, in our study, no significant difference was observed between the treated and control groups. However, *PR-1*, a marker of the SA signaling pathway, had significantly increased expression following inoculation with *B. cinerea*, suggesting that SA-mediated systemic resistance also plays a major role in the protection of 'Shine Muscat' against *B. cinerea*. When examining genes encoding enzymes involved in the degradation of cell walls, we found that inoculation with *B. cinerea* initially led to significantly

increased expression of *PME1*. These results suggest that shortly after inoculation, the enzyme PME, which is responsible for pectin demethylation, functioned at this stage. The initial degradation of pectin molecules was dominant, while at later stages, the elevated expression of the enzyme *PG1*, which is responsible for the cleavage of pectin molecules, further promoted the degradation of the cell wall, as exhibited by the softening of necrotic sites. Studies have shown that JA signaling plays an important role in the immunity of plants to necrotrophic pathogens^[25]. The expression of *LOX* and *COI1* significantly increased in the first and middle post-inoculation period, suggesting an increase in JA synthesis and consequently mediating the transcription of related genes to participate in the disease resistance process. The phenylpropane metabolic pathway is an important component of plant immunity by participating in the synthesis of substances such as lignans, flavonoids, and phenolics^[26], and increased levels of these compounds can improve the disease resistance of plants^[27,28]. In the present study, we found that in *PAL*, *4CL*, *STS*, *CHS*, *DFR*, and *UFGT* genes are significantly increased at the late stage of inoculation, which indicates that 'Shine Muscat' could be attempting to resist the invasion of *B. cinerea* through upregulation of the phenylpropanoid metabolic pathway, because of the combined action of multiple signals such as JA and H_2O_2 .

miR395 targets the *VvAPS1* gene and is involved in grape-*B. cinerea* interaction

MiRNAs are important regulatory components in plant growth and development, secondary metabolism, and response to biotic and abiotic stresses^[29,30]. MiRNAs and their target genes have been identified in grapes following cold stress, during growth and development^[31,32], and other pathogenic infections. However, it is still unknown whether miRNAs are involved specifically in the resistance of 'Shine Muscat' grapes against gray mold infestation. Therefore, in our study, miRNA libraries and degradome libraries were constructed using high-throughput sequencing to identify miRNAs and target genes in grapes under *B. cinerea* infestation. A total of 96 conserved miRNAs and 146 newly identified miRNAs from 42 families were identified, and with the aid of degradome sequencing, candidate targets of a total of 302 conserved and novel miRNAs were identified.

An increasing number of studies have shown that miRNAs are involved in plant-pathogen interactions, e.g., miR482^[33], miR159, and miR166^[34], etc. Through high-throughput sequencing, we found that *vvi-miR395* is involved in the interactions between 'Shine Muscat' and gray mold. miR395 levels first increased post-mold inoculation but then decreased after 12 h and onwards. Concurrently, *APS1*, the target gene of miR395, showed the opposite trend over the same time course, indicating a negative correlation between miR395 and *APS1*. We also found that miR395's candidate target gene *APS1* undergoes significant cleavage at the miR395 shear site through degradome sequencing, which was also confirmed by the results of 5' RACE experiments. Similarly, in rice, miR395 targets three genes, including *APS1*, *SULTR2;1*, and *SULTR2;2*, which in turn are involved in sulfur metabolism in rice, and the overexpression of miR395 significantly improved rice resistance^[17]. Furthermore, miR395 was found to target three ATP sulfurylase genes in *Arabidopsis* to regulate its sulfur metabolism^[35]. In another instance, miR395 was demonstrated to be directly involved in protecting *Arabidopsis* from oxidative damage during SO_2 exposure^[36]. We therefore hypothesized that in grapes, miR395 also affects the grape resistance to pathogens such as gray mold by regulating the grape's sulfur metabolism.

miR395 positively regulates grape disease resistance

In the present study, our analysis revealed that miR395 was involved in the interactions between grape and *B. cinerea*. To initially clarify the function of miR395 in the interactions, we performed transient overexpression experiments in *N. benthamiana*. The expression of pathogen response-related genes in the overexpression group showed a significant increase. In contrast, those in the silencing group showed different degrees of decreased expression of the same pathogen response genes. Correspondingly, the leaf inoculation experiments revealed that the disease spot area in the overexpression group was significantly smaller compared to the silencing group, which was also proved by Trypan Blue staining. In the related experiments after the transient transformation of grapes, the overexpression group showed significantly lower lesion diameters compared to the control group, demonstrating better disease resistance, while the silencing group had significantly higher lesion diameters than the control group. In exploring the internal reasons for this phenomenon, we found that in the overexpression group of miR395, the expression levels of pathogenic response-related genes, including *PR-1*, were significantly higher than those in the control, while in the silencing group, the opposite was true. Meanwhile, the expression level of genes such as *4CL* was also significantly affected, possibly generating more phenolic compounds through the phenylpropanoid metabolism pathway to respond to the invasion of gray mold. In addition, the overexpression group had a higher content of SO_4^{2-} and GSH, suggesting these compounds may be responsible for the high disease resistance of their grapes. Similarly, Md-miR395 was able to target the transcription factor MdWRKY26, regulate the expression of *PR* genes and participate in the interaction between apple cultivar Golden Delicious and *Alternaria alternaria* f. sp. *Mali*^[37].

vvi-miR395-APS1 functions in sulfate metabolism to modulate grape resistance against *B. cinerea*

In the present literature regarding sulfur metabolism, sulfur-containing compounds are considered to have direct antifungal effects^[38]. APS is an important gene in the plant sulfur metabolism pathway, in which its encoded ATP sulfatase catalyzes the reaction of sulfate ions with ATP to produce Adenosine-5'-Phosphosulfate (APS), which is an important starting point for plant sulfur assimilation. To further clarify the role of APS1 in this process, we performed a grape transient transformation assay with APS1, and confirmed its ability to negatively regulate the content of SO_4^{2-} . In addition, we found that it was negatively correlated with the content of GSH, which may be one of the ways in which it affects disease resistance, as GSH plays an important role in reducing oxidative damage in plants^[39,40]. Among the expression profiles of genes related to sulfur metabolism, *VvOASTL*, a gene encoding cysteine synthase, and *VvGS*, a gene encoding glutathione synthetase, were significantly increased in the *APS1* silencing group, which may have led to the increase of GSH content in the silencing group, in turn, affects the redox homeostasis of the cells, and plays a role in resisting the invasion of gray mold. In the study of rice *APS* genes, higher sulfate ion content resulted in higher resistance to pathogenic bacteria^[17]. This suggests that the content of sulfate ions also affects plant disease resistance. In addition, *4CL*, an important gene for phenylpropane metabolism, also showed a significant rise in the silencing group, suggesting that the phenylpropane metabolic pathway may also be up-regulated; meanwhile, the up-regulation of *PGIP*, *PIN*, and *PR-1* suggests that pathogen response-related genes are also affected. All the above phenotypic changes collectively altered the disease resistance abilities of grapes, indicating that *APS1* negatively regulated grapevine disease resistance to gray mold.

In conclusion, the results showed that after *B. cinerea* infests 'Shine Muscat' grapes, cells in the grapes generated a large amount

of ROS and induced expression of the phenylpropanoid metabolic pathway in response. Omics analysis and experiments have shown that miR395 negatively regulates the expression of the *APS1* gene, thereby regulating grape sulfur assimilation, promoting the accumulation of sulfate ions and GSH, and affecting the pathogen response-related genes of phenylpropane metabolism. This study elucidated the phenotypic and metabolic mechanisms underlying grape resistance to gray mold invasion and provided evidence supporting the involvement of the miR395-APS1 pathway in this resistance (Fig. 7). The interactions of miR395 with specific genes implicated in different pathogenic resistance mechanisms provide evidence to develop new concepts toward understanding the mechanisms of grape disease resistance. Future studies could involve sulfur supplementation or depletion experiments to further confirm the causal role of sulfur metabolism in resistance to gray mold. This research would deepen our understanding of sulfur's role in grape defense and could inform new strategies to reduce the incidence of gray mold.

Materials and methods

Plant materials and growth conditions

Grape clusters (*Vitis Labrusca* × *Vinifera* 'Shine Muscat') were collected from a vineyard in Hangzhou (Zhejiang Province, China). Samples were selected based on their similar appearance, size, and absence of lesions or other physiological defects. The grapes were transported to the laboratory within 2 h post-harvest. Upon arrival, they were immersed in a 5% (v/v) NaClO solution for 10 min, then rinsed three times in ultrapure water for 2 min each time. After washing, the grapes were air-dried in preparation for laboratory experiments and divided equally into groups, with five bunches per group. *Nicotiana benthamiana* plants used for gene transformation were grown in greenhouses with 16 h/8 h day/night at 25 °C.

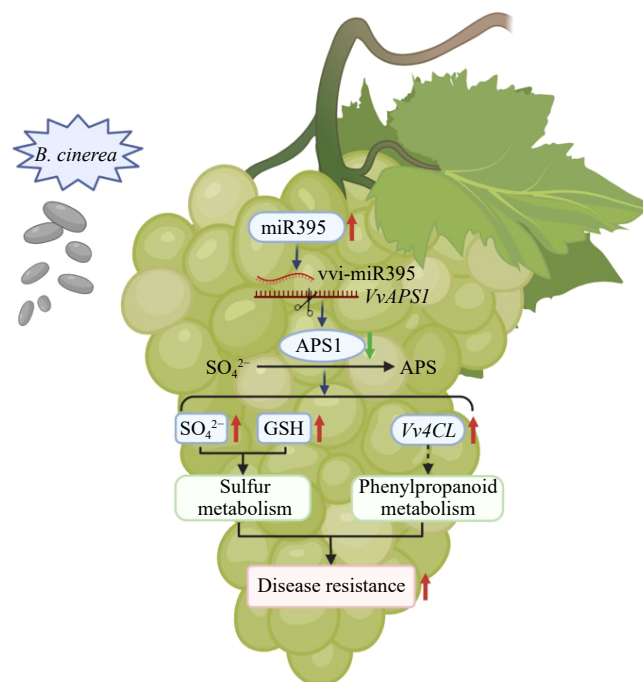


Fig. 7 A proposed model of the miR395-APS1 module enhancing resistance to *B. cinerea* via the sulfur metabolism pathway in 'Shine Muscat' grapes. Red arrows indicate upregulation, and green arrows indicate downregulation.

B. cinerea inoculation and analysis

B. cinerea strain B05.10 was cultured on PDA medium at 20 ± 1 °C. The conidial suspension was prepared and diluted to a concentration of 1.0×10^6 CFU. For inoculation, grapes were wounded with a sterile needle to a depth and diameter of 1 mm \times 1.5 mm, and 10 μ L of spore solution was applied to each wound^[6]. Control grapes received a mock inoculation with 0.01% (v/v) Triton X-100 solution. All samples were then incubated at 25 ± 1 °C with 90%–95% relative humidity. Tissues were collected from at least 10 berries per group at 0, 3, 6, 12, 24, 72, and 120 h after inoculation, immediately frozen in liquid nitrogen, and stored at -80 °C. Lesion diameter was measured and recorded every day after inoculation.

RNA extraction and RT-qPCR

Total RNA was isolated using the Plant Total RNA Isolation Kit Plus. Subsequently, cDNA was synthesized through reverse transcription using the HiScript III All-in-one RT SuperMix Perfect for qPCR kit^[6]. For miRNA synthesis, the miRNA 1st Strand cDNA Synthesis Kit (stem-loop method) was used. RT-qPCR analysis was performed with Taq Pro Universal SYBR qPCR Master Mix. All primers are listed in [Supplementary Table S1](#), and relative gene expression was calculated using the $2^{-\Delta\Delta CT}$ method^[6].

Small RNA and degradome libraries construction, sequencing, and analysis

Total RNA samples of grape tissues collected 72 h after inoculation were used for small RNA library construction, following Illumina's protocol. The libraries were sequenced on an Illumina HiSeq2500 by the Origin-gene (Shanghai, China), and miRNA sequences were identified using ACGT101-miR.

To identify mRNA targets, a degradome library was constructed from grape total RNA based on the method of German et al.^[41]. Analysis of miRNA targets was conducted using CleaveLand 4.0 and the ACGT101-DEG program. GO function annotation and KEGG pathway analysis of differential miRNA targets were performed using the GO and KEGG database, respectively.

Vector construction and plant transformation

The precursor and mature sequences of vvi-miR395 were obtained from miRBase. Potential target genes of vvi-miR395 were predicted using psRNATarget (www.zhaolab.org/psRNATarget). To generate the overexpression vector, primers for the vvi-miR395 precursor were designed using the NCBI Primer Design Tool ([Supplementary Table S1](#)), and the precursor sequence was amplified from grape genomic DNA. The PCR fragment was ligated into pNC-Cam2304-MCS35S using Nimble Cloning^[42]. The silencing vector for vvi-miR395 (STTM395) was designed and ligated into pNC-Cam2304-MCS35S following the method of Tang et al.^[43]. The *VvAPS1* overexpression and silencing vectors were constructed similarly. Target fragments were amplified with *VvAPS1* gene-specific primers, and the resulting PCR fragments were ligated into pNC-Cam2304-MCS35S and pNC-Cam2304-RNAi, respectively, using Nimble Cloning. All successfully constructed vectors were then transformed separately into *Agrobacterium tumefaciens* GV3101.

The grape transient transformation experiment was conducted following the method of Zhang et al.^[44]. 'Shine Muscat' grapes at the veraison stage were submerged in an *A. tumefaciens* suspension with an OD₆₀₀ of 1.0 and subjected to vacuum infiltration for 20 min. The grapes were then removed, dried with absorbent paper, incubated in the dark at 26 °C and 60% relative humidity for 24 h, and finally exposed to natural light. Samples were collected for qRT-PCR and gray mold inoculation experiments after 5 d.

Since the pathogenic gray mold in tobacco belongs to the same genus as that in grapes, tobacco leaves were chosen for preliminary

validation of vvi-miR395. Tobacco leaves were transiently transformed and then collected after 72 h of incubation at 25 °C with a 16 h/8 h day/night cycle for subsequent experiments. Detached leaf inoculation with gray mold was performed as described by Li et al.^[45]. After 72 h of transient transformation, undamaged leaves were collected, and sterile needles were used to create small wounds. Each wound site was inoculated with 20 μ L of gray mold spore suspension, and the leaves were placed on moist filter paper in Petri dishes. All samples were incubated at 25 ± 1 °C and 90%–95% relative humidity. Photographs were taken after 5 d to record the results.

Trypan blue staining was conducted using the method of Jiang et al.^[46]. Inoculated leaves were immersed in boiling Trypan Blue solution for 2 min, then soaked overnight. The leaves were subsequently decolorized multiple times with 70% chloral hydrate, followed by chlorophyll removal with 95% ethanol. The processed leaves were then stored and photographed.

Determination of physiological indexes

The levels of H₂O₂, O₂⁻, MDA, and GSSG were measured using their respective assay kits.

Similarly, the activities of the SOD, APX, and CAT enzymes were determined using SOD, APX, and CAT assay kits, respectively. All kits were obtained from Solarbio (Beijing, China). Due to the high moisture content of the samples, 0.2 g of frozen tissue powder was used for each assay.

5' RACE

The miR395 cleavage site on the *VvAPS1* transcript was identified using rapid amplification of 5'-cDNA ends (5' RACE) with the HiScript-TS 5'/3' RACE Kit. Total RNA was extracted using the Plant Total RNA Isolation Kit Plus. Primer sequences are listed in [Supplementary Table S1](#).

Subcellular localization assay

The amino acid sequence of the *VvAPS1* protein was analyzed by the WoLF PSORT database (www.genscript.com). The coding sequence without a stop codon of *VvAPS1* was amplified and cloned in the vector pNC-Cam1304-SubC and then introduced into tobacco leaf, using three plants as replicates. Primers are shown in [Supplementary Table S1](#).

Quantification of SO₄²⁻, SO₃²⁻, GSH, and cysteine contents

The quantification of SO₃²⁻ and SO₄²⁻ was performed following the method of Li et al.^[47].

The levels of GSH and cysteine (Cys) were measured using their respective assay kits (Solarbio, Beijing, China). All experiments were conducted according to the manufacturer's instructions, and due to the high moisture content of the samples, 0.2 g of frozen tissue powder was used for each assay.

Statistical analysis

The data are presented as the mean \pm SD from three biological and technical replicates, with each experiment performed in triplicate. Normality was assessed using the Shapiro-Wilk test. For data that deviated from normality, non-parametric tests, including the Kruskal-Wallis and Mann-Whitney U tests, were employed. All statistical analyses were conducted using SPSS 24.0 and GraphPad Prism 8.0.2, which was also used for data visualization. Significance levels were indicated as follows: * $p < 0.05$, ** $p < 0.01$, *** $p < 0.005$.

Accession numbers

The sequence data from this article have been deposited in the China National Center for Bioinformation (CNCB) database under accession numbers CRA020568 and CRA020572.

Author contributions

The authors confirm contribution to the paper as follows: experiment conception and design, experiment conduction, data analyses, draft manuscript preparation: Xiang Y, Yuan H; manuscript revision: Ma C, Li D, Hu Q, Dong Y, Kačániová M, Ban Z, Wu B, Li L. All authors contributed to the discussion, reviewed the results and approved the final version of the manuscript.

Data availability

The data supporting the findings of this study are available upon request. Additionally, the omics datasets have been deposited in the China National Center for Bioinformation (www.cncb.ac.cn) under the project code PRJCA032469. All data related to this manuscript and its supporting materials are available in this paper.

Acknowledgments

This work was supported by the National Natural Science Foundation of China (Grant Nos U2003213 and 32472399) and the Key Research and Development Program of Zhejiang Province (Grant No. 2021C02015) for financial support.

Conflict of interest

The authors declare that they have no conflict of interest.

Supplementary information accompanies this paper at (<https://www.maxapress.com/article/doi/10.48130/fia-0025-0002>)

Dates

Received 1 August 2024; Revised 24 November 2024; Accepted 30 December 2024; Published online 23 January 2025

References

- Wang L, Luo Z, Yang M, Li D, Qi M, et al. 2020. Role of exogenous melatonin in table grapes: First evidence on contribution to the phenolics-oriented response. *Food Chemistry* 329:127155
- Yamada M, Yamane H, Sato A, Hirakawa N, Iwanami H, et al. 2008. New grape cultivar 'Shine Muscat'. *Bulletin of the National Institute of Fruit Tree Science* 7:21–38
- Lim YS, Hassan O, Chang T. 2019. First report of anthracnose of shine muscat caused by *Colletotrichum fructicola* in Korea. *Mycobiology* 49:183–87
- Dean R, Van Kan JAL, Pretorius ZA, Hammond-Kosack KE, Di Pietro A, et al. 2012. The Top 10 fungal pathogens in molecular plant pathology. *Molecular Plant Pathology* 13:414–30
- Zhou H, Xie Y, Wu T, Wang X, Gao J, et al. 2024. Cork taint of wines: the formation, analysis, and control of 2,4,6-trichloroanisole. *Food Innovation and Advances* 3:111–25
- Xiang Y, Yuan H, Mao M, Hu Q, Dong Y, et al. 2024. Reciprocal inhibition of autophagy and *Botrytis cinerea*-induced programmed cell death in 'Shine Muscat' grapes. *Food Chemistry* 460:140512
- Zhang Z, Zhao P, Zhang P, Su L, Jia H, et al. 2020. Integrative transcriptomics and metabolomics data exploring the effect of chitosan on postharvest grape resistance to *Botrytis cinerea*. *Postharvest Biology and Technology* 167:111248
- Romanazzi G, Lichter A, Gabler FM, Smilanick JL. 2012. Recent advances on the use of natural and safe alternatives to conventional methods to control postharvest gray mold of table grapes. *Postharvest Biology and Technology* 63:141–47
- Zhang P, Jia H, Gong P, Sadeghnezhad E, Pang Q, et al. 2021. Chitosan induces jasmonic acid production leading to resistance of ripened fruit against *Botrytis cinerea* infection. *Food Chemistry* 337:127772
- Xu J, Zhang Z, Li X, Wei J, Wu B. 2019. Effect of nitrous oxide against *Botrytis cinerea* and phenylpropanoid pathway metabolism in table grapes. *Scientia Horticulturae* 254:99–105
- Song Z, Pang Q, Lu S, Yu L, Pervaiz T, et al. 2022. Transcriptomic and metabolomic approaches to counter the effect of *Botrytis cinerea* in grape berry with the application of nitric oxide. *Scientia Horticulturae* 296:110901
- Xu D, Deng Y, Han T, Jiang L, Xi P, et al. 2018. In vitro and in vivo effectiveness of phenolic compounds for the control of postharvest gray mold of table grapes. *Postharvest Biology and Technology* 139:106–14
- Raynaldo FA, Xu Y, Yolandanani, Wang Q, Wu B, et al. 2024. Biological control and other alternatives to chemical fungicides in controlling postharvest disease of fruits caused by *Alternaria alternata* and *Botrytis cinerea*. *Food Innovation and Advances* 3:135–43
- Djami-Tchatchou AT, Sanan-Mishra N, Ntushelo K, Dubery IA. 2017. Functional roles of microRNAs in agronomically important plants — potential as targets for crop improvement and protection. *Frontiers in Plant Science* 8:378
- Dong Y, Tang M, Huang Z, Song J, Xu J, et al. 2022. The miR164a-NAM3 module confers cold tolerance by inducing ethylene production in tomato. *The Plant Journal* 111:440–56
- Peláez P, Sanchez F. 2013. Small RNAs in plant defense responses during viral and bacterial interactions: similarities and differences. *Frontiers in Plant Science* 4:343
- Yang Z, Hui S, Lv Y, Zhang M, Chen D, et al. 2022. miR395-regulated sulfate metabolism exploits pathogen sensitivity to sulfate to boost immunity in rice. *Molecular Plant* 15:671–88
- Tian X, Song L, Wang Y, Jin W, Tong F, et al. 2018. miR394 acts as a negative regulator of *Arabidopsis* resistance to *B. cinerea* infection by targeting LCR. *Frontiers in Plant Science* 9:903
- Wu F, Qi J, Meng X, Jin W. 2020. miR319c acts as a positive regulator of tomato against *Botrytis cinerea* infection by targeting TCP29. *Plant Science* 300:110610
- Val-Torregrosa B, Bundó M, Martín-Cardoso H, Bach-Pages M, Chiou TJ, et al. 2022. Phosphate-induced resistance to pathogen infection in *Arabidopsis*. *The Plant Journal* 110:452–69
- Bolwell GP, Daudi A. 2009. Reactive oxygen species in plant–pathogen interactions. In *Reactive Oxygen Species in Plant Signaling*, eds. Rio L, Puppo A. Berlin, Heidelberg: Springer. pp. 113–33. doi: 10.1007/978-3-642-00390-5_7
- Lamb C, Dixon RA. 1997. The oxidative burst in plant disease resistance. *Annual Review of Plant Physiology and Plant Molecular Biology* 48:251–75
- Tsuda K, Katagiri F. 2010. Comparing signaling mechanisms engaged in pattern-triggered and effector-triggered immunity. *Current Opinion in Plant Biology* 13:459–65
- Silva KJP, Mahna N, Mou Z, Folta KM. 2018. *NPR1* as a transgenic crop protection strategy in horticultural species. *Horticulture Research* 5:15
- Chico J-M, Fernández-Barbero G, Chini A, Fernández-Calvo P, Díez-Díaz M, et al. 2014. Repression of Jasmonate-Dependent Defenses by Shade Involves Differential Regulation of Protein Stability of MYC Transcription Factors and Their JAZ Repressors in *Arabidopsis*. *The Plant Cell* 26:1967–80
- Vogt T. 2010. Phenylpropanoid biosynthesis. *Molecular Plant* 3:2–20
- Ge Y, Duan B, Li C, Tang Q, Li X, et al. 2018. γ -Aminobutyric acid delays senescence of blueberry fruit by regulation of reactive oxygen species metabolism and phenylpropanoid pathway. *Scientia Horticulturae* 240:303–9
- Yao H, Tian S. 2005. Effects of pre- and post-harvest application of salicylic acid or methyl jasmonate on inducing disease resistance of sweet cherry fruit in storage. *Postharvest Biology and Technology* 35:253–62
- Liu R, Lai B, Hu B, Qin Y, Hu G, et al. 2017. Identification of microRNAs and their target genes related to the accumulation of anthocyanins in *Litchi chinensis* by high-throughput sequencing and degradome analysis. *Frontiers in Plant Science* 7:2059
- Xie Z, Wang A, Li H, Yu J, Jiang J, et al. 2017. High throughput deep sequencing reveals the important roles of microRNAs during sweet-potato storage at chilling temperature. *Scientific Reports* 7:16578
- Rooy SSB, Ghabooli M, Salekdeh GH, Fard EM, Karimi R, et al. 2023. Identification of novel cold stress responsive microRNAs and their putative targets in 'Sultana' grapevine (*Vitis vinifera*) using RNA deep sequencing. *Acta Physiologiae Plantarum* 45:2

32. Wang C, Leng X, Zhang Y, Kayesh E, Zhang Y, et al. 2014. Transcriptome-wide analysis of dynamic variations in regulation modes of grapevine microRNAs on their target genes during grapevine development. *Plant Molecular Biology* 84:269–85
33. Shivaprasad PV, Chen HM, Patel K, Bond DM, Santos BACM, et al. 2012. A microRNA superfamily regulates nucleotide binding site–Leucine-rich repeats and other mRNAs. *The Plant Cell* 24:859–74
34. Zhang T, Zhao YL, Zhao JH, Wang S, Jin Y, et al. 2016. Cotton plants export microRNAs to inhibit virulence gene expression in a fungal pathogen. *Nature Plants* 2:16153
35. Matthewman CA, Kawashima CG, Húska D, Csorba T, Dalmay T, Kopriva S. 2012. miR395 is a general component of the sulfate assimilation regulatory network in Arabidopsis. *FEBS Letters* 586:3242–48
36. Li L, Yi H, Xue M, Yi M. 2017. miR398 and miR395 are involved in response to SO₂ stress in *Arabidopsis thaliana*. *Ecotoxicology* 26:1181–87
37. Zhang Q, Li Y, Zhang Y, Wu C, Wang S, et al. 2017. Md-miR156ab and Md-miR395 target WRKY transcription factors to influence apple resistance to leaf spot disease. *Frontiers in Plant Science* 8:526
38. Bloem E, Haneklaus S, Schnug E. 2015. Milestones in plant sulfur research on sulfur-induced-resistance (SIR) in Europe. *Frontiers in Plant Science* 5:779
39. Chen Y, Li Z, Ettoumi FE, Li D, Wang L, et al. 2022. The detoxification of cellular sulfite in table grape under SO₂ exposure: Quantitative evidence of sulfur absorption and assimilation patterns. *Journal of Hazardous Materials* 439:129685
40. Ghanta S, Bhattacharyya D, Chattopadhyay S. 2011. Glutathione signaling acts through NPR1-dependent SA-mediated pathway to mitigate biotic stress. *Plant Signaling & Behavior* 6:607–9
41. German MA, Pillay M, Jeong DH, Hetawal A, Luo S, et al. 2008. Global identification of microRNA–target RNA pairs by parallel analysis of RNA ends. *Nature Biotechnology* 26:941–46
42. Yan P, Zeng Y, Shen W, Tuo D, Li X, et al. 2020. Nimble cloning: a simple, versatile, and efficient system for standardized molecular cloning. *Frontiers in Bioengineering and Biotechnology* 7:460
43. Tang G, Yan J, Gu Y, Qiao M, Fan R, et al. 2012. Construction of short tandem target mimic (STTM) to block the functions of plant and animal microRNAs. *Methods* 58:118–25
44. Zhang PF, Dong YM, Wen HY, Liang CM, Niu TQ, et al. 2020. Knockdown of VvMYBA1 via virus-induced gene silencing decreases anthocyanin biosynthesis in grape berries. *Canadian Journal of Plant Science* 100:175–84
45. Li JB, Luan YS, Liu Z. 2015. SpWRKY1 mediates resistance to *Phytophthora infestans* and tolerance to salt and drought stress by modulating reactive oxygen species homeostasis and expression of defense-related genes in tomato. *Plant Cell, Tissue and Organ Culture (PCTOC)* 123:67–81
46. Jiang N, Meng J, Cui J, Sun G, Luan Y. 2018. Function identification of miR482b, a negative regulator during tomato resistance to *Phytophthora infestans*. *Horticulture Research* 5:9
47. Li Z, Chen S, Qi M, Yang M, Yuan H, et al. 2023. Inhibition of postharvest rachis browning of table grapes by sulfur dioxide: Evidence from phenolic metabolism and sulfur assimilation. *Postharvest Biology and Technology* 204:112413



Copyright: © 2025 by the author(s). Published by Maximum Academic Press on behalf of China Agricultural University, Zhejiang University and Shenyang Agricultural University. This article is an open access article distributed under Creative Commons Attribution License (CC BY 4.0), visit <https://creativecommons.org/licenses/by/4.0/>.